

The jump effect of a general eccentric cylinder rolling on a ramp

E. Aldo Arroyo^{(a)*} and M. Aparicio Alcalde^{(b)†}

^(a)Centro de Ciências Naturais e Humanas, Universidade Federal do ABC,
Santo André, 09210-170 São Paulo, SP, Brazil.

^(b)Instituto de Ciências Exatas e Tecnológicas, Universidade Federal de Viçosa,
38810-000, Rio Paranaíba, MG, Brazil.

May 3, 2023

Abstract

Interesting phenomena occur when an eccentric rigid body rolls on an inclined or horizontal plane. For example, a variety of motions between rolling and sliding are exhibited until suddenly a jump occurs. We provide a detailed theoretical description of the jump effect for a general eccentric cylinder. Before the jump, when the cylinder moves along the ramp, we can assume a pure rolling motion. However, it turns out that when the cylinder reaches its jumping position, both the normal and static frictional forces approach zero. Thus, it seems that there will no longer be sufficient force to maintain rolling without slip. In order to have a jump without slipping, we prove that the parameters that characterize the dynamic behavior of the cylinder must belong to some restricted region.

1 Introduction

The physical system consists of a rigid body, such as hoops, wheels, disks, and spheres, whose center of mass is located at a distance $d \neq 0$ from the geometric center and rolls on a horizontal or inclined plane with friction. This system has interesting and unexpected dynamic behavior, which has attracted the attention of the community. In Fig. 1, a general configuration of the physical system is exhibited, where we can identify an inclined ramp making an angle α with the horizontal, and a cylinder of radius R with its center of mass located at a distance d from the geometric center. The cylinder rolls over the ramp, and its motion is tracked by the angle θ .

In the case of a horizontal plane (i.e., $\alpha = 0^\circ$), there is literature on the dynamics of a particular cylinder. This cylinder consists of a very thin, massless cylindrical shell with a point mass stuck to its surface. The motion of this cylinder has been studied and debated by several authors [1, 2]. When the point mass attached to the cylinder is initially at the highest point of the cylinder, and the system is released from rest (i.e., the initial conditions are such that $\theta_0 = 0$ and $\dot{\theta}_0 = 0$), Tokieda [2] showed that the cylinder must jump at $\theta = 90^\circ$. However, subsequent articles have shown that the assumption made by the author, that the jump happens immediately after the pure rolling motion, is incorrect. For instance, it has been shown that before the jump, there must be sliding [3, 4, 5]. Despite this fact, Pritchett [4] obtained numerical and experimental results (for a hula hoop with a stuck point mass) showing that the jump happens around $\theta = 90^\circ$, even when considering slippage.

*aldo.arroyo@ufabc.edu.br

†aparicio@ufv.br

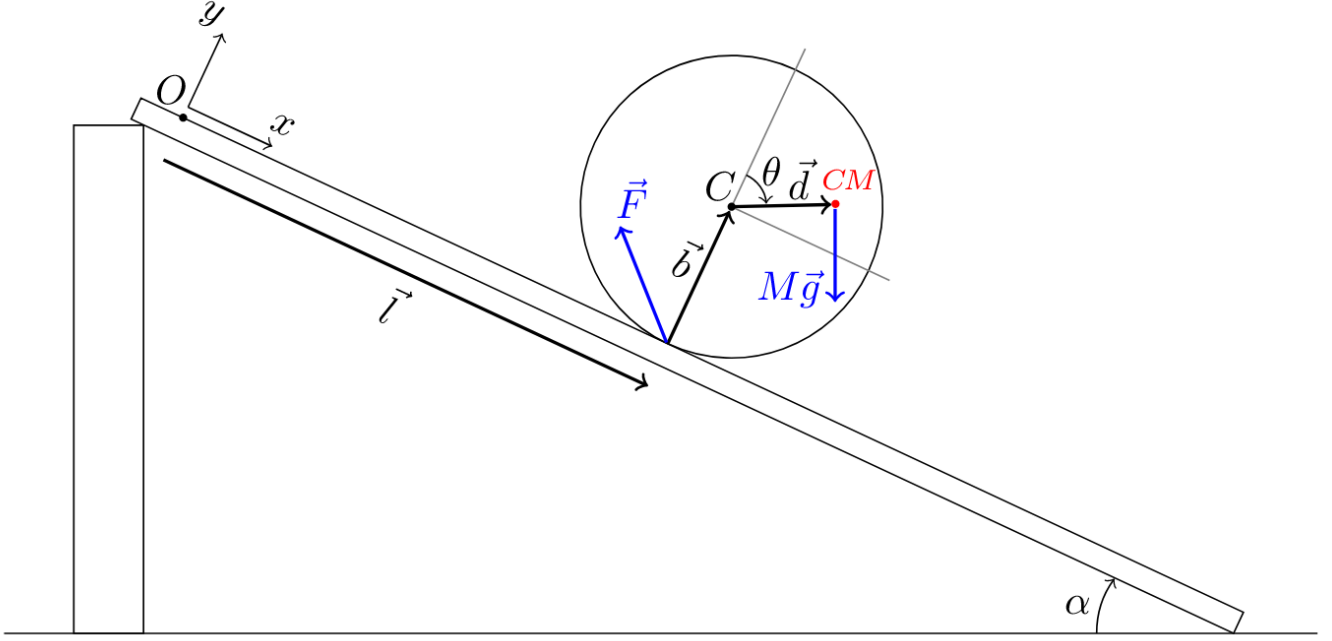


Figure 1: Schematic configuration of the physical system showing a cylinder rolling down a ramp of angle α . The position of the geometric center C , and the center of mass CM of the cylinder with respect to point O are given by the vectors $\vec{l} + \vec{b}$ and $\vec{l} + \vec{b} + \vec{d}$, respectively. The vector \vec{F} represents the force acting at the contact point between the cylinder and the ramp, and $M\vec{g}$ is the cylinder's weight.

Moreover, to test the jump at this angle of 90° , Theron [6] claimed that the elasticity of the hula hoop must be considered. As observed, despite the physical system being simple, the motion of the cylinder turns out to be, in general, complex. Further analysis has shown that a variety of these motions can include self-induced jumping motions [7, 8, 9, 10, 11], as well as multiple transitions back and forth from rolling to slipping [12, 13, 14, 15].

In the case of an inclined plane (i.e., $\alpha \neq 0$), we have found a few models that consider this case. One of them studied an eccentric wheel [6], and the other studied an eccentric disk [16]. These works hypothesize that the wheel (or disk) must slip before jumping. Other references [17, 18, 19, 20] have studied the equations of motion for this cylinder by means of the Lagrangian formulation or a cumbersome torque analysis. However, these works did not determine the position where the cylinder jumps.

In all the references we have found (with the exception of [21]), it was assumed that the necessary condition for the jump is when the normal force F_y (acting perpendicularly from the ramp over the cylinder) vanishes at the instant of the hop. Let us remark that a different jump condition will be used in this work, and this condition turns out to be equivalent to that of [21]. As argued in reference [21], the equation that the angle θ and the angular velocity $\dot{\theta}$ must satisfy at the position where the cylinder jumps are given by

$$-g \cos \alpha + d \dot{\theta}^2 \cos \theta = 0. \quad (1)$$

Assuming pure rolling motion, which implies conservation of energy, and using the initial conditions $\theta_0 = 0$ and $\dot{\theta}_0 = 0$, it was possible to find an angle θ_J that is a solution of Eq. (1). Consequently, the position $l_J = R\theta_J$ along the inclined plane where the cylinder jumps can be determined. However, there is a subtlety in the pure rolling assumption. For a given value of the coefficient of static friction μ_s between the cylinder and inclined plane, before the cylinder reaches the position determined by the angle θ_J , it may happen that the static friction exceeds its maximum value. This would imply that the cylinder slips before jumping.

Therefore, aside from the jump condition issue, we remark that there is an important open question: Are there cases where an eccentric rigid body rolling on an inclined (or horizontal) plane jumps just after pure rolling motion? As we are going to see, the answer to this question is not trivial and depends on the values of μ_s , the angle α , and the moment of inertia of the rigid body considered. A general body that encompasses all types of eccentric bodies having a cylindrical shape will be referred to as a general eccentric cylinder. It turns out that the dynamic characteristics of this cylinder can be parameterized using two parameters, χ and k_m . By exploring this generality that we consider in our work, we prove that there are (quite common) situations in which the jump occurs immediately after sliding roll, and there are (less common) situations where the jump occurs immediately after pure rolling. We also prove that when the jump occurs immediately after sliding roll, we have $F_y = 0$, and in the cases where the jump occurs immediately after pure rolling, we have $F_y > 0$. Therefore, it would be correct to consider $F_y = 0$ as a necessary condition for the jump whenever there is sliding rolling immediately before the jump, as occurs in many studies in the literature, but it would be incorrect to state the same when the jump occurs immediately after pure rolling or in general cases.

This paper is organized as follows. In section 2, we will describe the physical system to be analyzed and derive the corresponding equations of motion. Then we will propose a model for the general eccentric cylinder. In section 3, we determine the region where the parameters that characterize the dynamical behavior of the general eccentric cylinder must belong in order to have a jump without slip, for any value of α and μ_s . In section 4, we will provide a summary and suggest further directions for exploration.

2 Description of the system and derivation of the equations of motion

In this section, we will define the physical system to be studied and derive the corresponding equations of motion. The mechanical system consists of a general eccentric cylinder rolling down an inclined ramp, as shown in Fig. 1. The term eccentric means that the center of mass is located at a distance of d from the geometric center. By general, we mean that the mass distribution within the cylinder is arbitrary, with the only restriction being that this distribution is invariant under translations along the z -axis. Throughout the motion, we will assume that the principal axis of the cylinder passing through point C always remains parallel to the z -axis. Note that when the cylinder's height is very small compared to the radius, the cylinder represents a disk, and if the mass distribution is concentrated on the edge, the cylinder becomes a hoop or wheel. In this sense, we can say that this general eccentric cylinder can encompass all types of eccentric bodies that have cylindrical shape.

In Fig. 1, we also show the coordinate system xy , where the origin is set at the point O located at the top of the ramp. The x -axis and y -axis are parallel and perpendicular to the ramp, respectively. The position of the center of mass with respect to the geometric center of the cylinder is given by the vector

$$\vec{d} = d \sin \theta \hat{i} + d \cos \theta \hat{j}, \quad (2)$$

where θ is the angle between the vector \vec{d} and the y -axis.

Using the coordinate system xy , which is an inertial reference frame, we can write the position of the center of mass as follows

$$\vec{r}_{CM} = \vec{l} + \vec{b} + \vec{d} = (l + d \sin \theta) \hat{i} + (b + d \cos \theta) \hat{j}. \quad (3)$$

In the case where the cylinder remains in contact with the ramp, the vector \vec{b} is given by $\vec{b} = R \hat{j}$, where R is the radius of the cylinder. While in the case where the cylinder loses contact with the ramp and flies, we have $|\vec{b}| > R$.

The two equations that are used to determine the dynamics of this rigid body are:

(i) Newton's second law for the motion of the center of mass:

$$\vec{F}_T = M\ddot{\vec{r}}_{CM}, \quad (4)$$

where the subscript T means that we are considering the total force acting on the cylinder; and

(ii) Newton's second law for rotations:

$$\vec{\tau}_T = I_{CM}\ddot{\vec{\theta}}, \quad (5)$$

where $\ddot{\vec{\theta}}$ is defined as $\ddot{\vec{\theta}} = -\ddot{\theta}\hat{k}$, and the total torque $\vec{\tau}_T$ and moment of inertia I_{CM} are taken around the center of mass.

From the configuration of the system shown in Fig. 1, we can write Eq. (5) as follows:

$$-(\vec{b} + \vec{d}) \times \vec{F} = -I_{CM}\ddot{\theta}\hat{k}. \quad (6)$$

Since the total force acting on the cylinder is given by $\vec{F}_T = \vec{F} + M\vec{g}$, using Eqs. (3) and (4), we obtain

$$\vec{F} = M(\ddot{\vec{l}} + \ddot{\vec{b}} + \ddot{\vec{d}} - \vec{g}). \quad (7)$$

Let us write the force \vec{F} in terms of its components in the directions of the x and y -axis

$$\vec{F} = F_x\hat{i} + F_y\hat{j}, \quad (8)$$

note that these components F_x and F_y are the friction and normal force, respectively. Now substituting Eqs. (3) and (8) into Eq. (7), we get

$$\begin{aligned} F_x &= M\ddot{l} + Md(\sin\theta)'' - Mg\sin\alpha, \\ F_y &= M\ddot{b} + Md(\cos\theta)'' + Mg\cos\alpha. \end{aligned} \quad (9)$$

Using Eqs. (2), (8) and writing $\vec{b} = b\hat{j}$, from Eq. (6) we obtain

$$I_{CM}\ddot{\theta} = d\sin\theta F_y - (b + d\cos\theta)F_x. \quad (10)$$

The equations (9) and (10) will be useful in analyzing three possible types of motion for the cylinder: pure rolling, rolling with slipping, and flight motion. For each type of motion, additional relations between the forces and positions must be established. In the next two subsections, we will study the equations in the case of pure rolling and flight motion.

2.1 Equations in the case of pure rolling motion

Since the cylinder is in contact with the ramp, we have $b = R$, which means that b is constant and, therefore, $\ddot{b} = 0$. Moreover, due to the pure rolling condition, we also have $l = l_0 + R(\theta - \theta_0)$, and consequently $\ddot{l} = R\ddot{\theta}$. The moments of inertia I_C and I_{CM} with respect to the geometric center C and the center of mass CM of the cylinder are related by the equation $I_C = I_{CM} + Md^2$. Substituting these equations into Eqs. (9) and (10), we can derive the following nonlinear second-order differential equation

$$\ddot{\theta} \left(\frac{I_C}{MR^2} + 1 + 2\chi\cos\theta \right) - \chi\dot{\theta}^2\sin\theta - \frac{g}{R}(\chi\sin(\alpha + \theta) + \sin\alpha) = 0, \quad (11)$$

where we have defined the following dimensionless parameter χ as follows

$$\chi = \frac{d}{R}. \quad (12)$$

2.2 Equations in the case of flight motion

In the case of flight motion, the cylinder has no contact with the ramp, therefore the contact force is null, i.e., $F_x = F_y = 0$. From Eq. (10) it is straightforward to show that the angular velocity $\dot{\theta}$ is constant. And from Eq. (9) we obtain:

$$\begin{aligned}\ddot{l} &= d\dot{\theta}^2 \sin \theta + g \sin \alpha, \\ \ddot{b} &= d\dot{\theta}^2 \cos \theta - g \cos \alpha.\end{aligned}\tag{13}$$

These equations are consistent with the common knowledge about the free-fall motion of a rigid body, where the center of mass performs a parabolic trajectory and the angular velocity is constant.

2.3 Transition from rolling to flight motion

In order to understand the condition for the transition from rolling to flight motion, we will perform the following analysis. Before the jump, the cylinder stays in contact with the ramp, so $b(t) = R$, $\dot{b}(t) = \ddot{b}(t) = 0$, and the values of $\theta(t)$, $\dot{\theta}(t)$, and $\ddot{\theta}(t)$ are related by means of Eq. (10). At the moment of the jump, the values of $b(t)$, $\theta(t)$, $\dot{b}(t)$, and $\ddot{\theta}(t)$ change continuously. The continuity of $\dot{b}(t)$ and $\dot{\theta}(t)$ is supported by the fact that there are no additional external forces acting on the cylinder at the instant of the jump that would change the cylinder's momentum.

After the jump, the cylinder performs a flight motion where the relations in Eq. (13) are valid. Due to the continuities mentioned above, the values of $b = R$ and $\dot{b} = 0$ are the initial conditions for $b(t)$ in the flight motion. Therefore, when the value of \ddot{b} given by Eq. (13) starts to be greater than zero, it implies that the values of \dot{b} and b start to increase. It is interesting to note that this increase in the values of \dot{b} and b happens because we assumed that the cylinder is not attached to the ramp. Consequently, at the point where the transition from rolling to flight motion occurs, we must have $\ddot{b} = 0$ in Eq. (13). This condition means ¹:

$$d\dot{\theta}^2 \cos \theta - g \cos \alpha = 0.\tag{14}$$

Before the jump, in order to understand the behavior of \ddot{b} as defined in Eq. (13), we need to track the value of $\dot{\theta}$. The motion of the cylinder starts with $\dot{\theta} = 0$, and due to the action of gravity, $\dot{\theta}$ increases. Therefore, at the beginning, $\ddot{b} = -g \cos \alpha < 0$, and subsequently, \ddot{b} increases because of the contribution of $\dot{\theta}^2$ (with some oscillation due to the factor $\cos \theta$). This implies that at some future instant, when \ddot{b} approaches zero, i.e., when Eq. (14) is satisfied, we reach the moment when the cylinder jumps.

Let us comment that in other works [5, 6, 16], the jump condition has been given by $F_y = 0$. Namely, the jump happens at the point where the normal force vanishes. However, these works consider the hypothesis that the jump is not possible from pure rolling, which means that the cylinder must slide before jumping. Although the main focus of our work is not on the slip case, using equations (9) and (10), together with the relation $F_x = \sigma \mu_k F_y$, where μ_k is the coefficient of kinetic friction, and $\sigma = -1$ in case $\dot{l} > R\dot{\theta}$ (i.e., skidding motion) and $\sigma = +1$ in case $\dot{l} < R\dot{\theta}$ (i.e., spinning motion), we can show that the normal force F_y is given by

$$F_y = \frac{M I_{CM} (d\dot{\theta}^2 \cos \theta - g \cos \alpha)}{M d (\sigma \mu_k \sin \theta (d \cos \theta + R) - d \sin^2 \theta) - I_{CM}}.\tag{15}$$

From Eq. (15), we observe that the jump condition, as given by Eq. (14), clearly implies that the normal force F_y vanishes. It should be noted that the expression for the normal force, as given by Eq. (15), is only valid when there is slippage. If the jump occurs from pure rolling motion, employing Eq. (14), we will show that the normal force does not necessarily vanish.

¹This jump condition was obtained in Ref. [21] using an alternative approach.

2.4 Scale invariance of the dynamics and a model for the general eccentric cylinder

Considering a general mass distribution inside the cylinder, with the only restriction being that this distribution is invariant under translations along the cylinder's principal axis, such that the center of mass does not coincide with the cylinder's geometric center, in this subsection we analyze the equations of motion of this general eccentric cylinder. It turns out that the equations of motion have scale invariance. By using this invariance, we can find common characteristics between two different cylinders in a way that the dynamics of both cylinders are equivalent. These common characteristics between two different cylinders can be parameterized using two independent parameters. We also propose a simplified model of the eccentric cylinder where the two independent parameters have a simple geometric and mass distribution interpretation. We prove that this simplified model is dynamically equivalent to any general cylinder considered in our study.

Let us consider a cartesian coordinate system fixed to the cylinder, such that the z -axis coincides with the principal axis, and the coordinate origin is located at the cylinder's geometric center C . The center of mass CM and the cylinder's moment of inertia with respect to the z -axis are computed as $\vec{r}_{CM} = \frac{1}{M} \int dx dy dz \vec{r} \rho(x, y)$ and $I_C = \int dx dy dz (x^2 + y^2) \rho(x, y)$, respectively, where $\rho(x, y)$ is the mass density bounded by the cylindrical surface. Since the mass distribution is invariant under translations along the z -axis, the density $\rho(x, y)$ does not depend on z . These specifications provide two general implications:

1. The CM can be located at any distance d from the cylinder's geometric center C , with this distance restricted to the interval $d \in [0, R]$. For example, the particular case where $d = R$ occurs when the entire cylinder's mass is distributed along a line on the cylindrical lateral surface that is parallel to the z -axis.
2. For fixed values of M , R , and d , the moment of inertia I_{CM} (or equivalently I_C , thanks to the relation $I_C = I_{CM} + Md^2$), has minimum and maximum values, where these bounding values are:
 - (a) *The minimum:* this value corresponds to the case where the whole cylinder's mass is distributed along a line (parallel to the z -axis) that passes through the CM , therefore in this case we have: $I_{CM} = 0$ or $I_C = Md^2$.
 - (b) *The maximum:* this value corresponds to the case where the whole cylinder's mass is distributed on the cylinder's lateral surface, so in this case we have: $I_{CM} = MR^2 - Md^2$ or $I_C = MR^2$.

Given a value of I_C such that $Md^2 \leq I_C \leq MR^2$, there are a variety of possibilities for the mass distribution $\rho(x, y)$ that yield the same value of I_C . Since for a fixed values of M , R , d and g , the equations of motion, given by Eqs. (9) and (10), depend only on I_C , the cylinder's dynamical behavior does not depend on specific details of the mass distribution $\rho(x, y)$.

From Eqs. (9) and (10), we can write the following equation

$$\tilde{I}_{CM} \frac{d^2 \tilde{\theta}}{d\tilde{t}^2} = \chi \sin \tilde{\theta} \left(\frac{d^2 \tilde{b}}{d\tilde{t}^2} + \chi \frac{d^2 \cos \tilde{\theta}}{d\tilde{t}^2} + \cos \alpha \right) - (\tilde{b} + \chi \cos \tilde{\theta}) \left(\frac{d^2 \tilde{l}}{d\tilde{t}^2} + \chi \frac{d^2 \sin \tilde{\theta}}{d\tilde{t}^2} - \sin \alpha \right), \quad (16)$$

where we have defined the adimensional quantities $\tilde{I}_{CM} = \frac{I_{CM}}{MR^2}$, $\tilde{t} = \sqrt{\frac{g}{R}} t$, $\tilde{\theta} = \theta$, $\tilde{b} = b/R$, $\tilde{l} = l/R$ and χ is given by Eq. (12). The functions $\tilde{\theta}$, \tilde{b} , and \tilde{l} are related to the solutions θ , b , and l of the equations of motion. More explicitly, these relations are given by $\theta(t) = \tilde{\theta}(\sqrt{\frac{g}{R}} t)$, $b(t) = R\tilde{b}(\sqrt{\frac{g}{R}} t)$, and $l(t) = R\tilde{l}(\sqrt{\frac{g}{R}} t)$. At this point, we are ready to analyze the dependence of the cylinder's dynamics with respect to M and R . Consider two cylinders, one with mass and radius given by the set (M, R)

and the other by (M', R') . If χ and \tilde{I}_{CM} are the same for both cylinders, then due to Eq. (16), they share the same solutions $\tilde{\theta}$, \tilde{b} , and \tilde{l} . Therefore, the set of functions (θ', b', l') and (θ, b, l) are related by $\theta' = \theta$, $b' = \frac{R'}{R}b$, $l' = \frac{R'}{R}l$. Namely, θ is equal for both sets, while b and l do not depend on M and scale by a factor proportional to R . Similarly, since $t = \sqrt{\frac{R}{g}}\tilde{t}$, the time of the events that happen throughout the motion (like the time when the jump happens) scales by a factor proportional to the square root of R .

From the above observations, and defining the scale factor $\lambda = \frac{R'}{R}$, we conclude that the equations of motion are invariant under the scale transformation $\theta' = \theta$, $b' = \lambda b$, $l' = \lambda l$, $t' = \sqrt{\lambda}t$ provided that χ and \tilde{I}_{CM} are the same for the two different sets of values (M, R) and (M', R') . Since $\chi = \chi'$, we have that $d' = \lambda d$. Furthermore, from $\tilde{I}_{CM} = \tilde{I}'_{CM}$, namely $\frac{I_{CM}}{MR^2} = \frac{I'_{CM}}{M'R'^2}$, or $\frac{I_C}{MR^2} = \frac{I'_C}{M'R'^2}$, and using $I_C = \int dx dy dz (x^2 + y^2)\rho(x, y)$, we get the relation

$$\int dx dy dz \left(\left(\frac{x}{R} \right)^2 + \left(\frac{y}{R} \right)^2 \right) \frac{\rho(x, y)}{M} = \int dx' dy' dz' \left(\left(\frac{x'}{R'} \right)^2 + \left(\frac{y'}{R'} \right)^2 \right) \frac{\rho'(x', y')}{M'},$$

which means that under the transformation $(x', y', z') = (\lambda x, \lambda y, \lambda z)$, and the change of mass from M to M' , we have that $\frac{\rho(x, y)}{M} dx dy dz = \frac{\rho'(x', y')}{M'} dx' dy' dz'$, or $\frac{dm}{M} = \frac{dm'}{M'}$, that is the mass densities (divided by the total mass) of the cylinders are related by $\frac{\rho(x, y)}{M} = \lambda^3 \frac{\rho'(x', y')}{M'}$.

A summary of the previous analysis is as follows: given two different cylinders, where to calculate their centers of mass and moments of inertia, we use cartesian coordinate systems fixed to them. Let (x', y', z') the coordinate system fixed to one cylinder, and (x, y, z) to the other one. If these coordinate systems are related by the scale transformation $(x', y', z') = (\lambda x, \lambda y, \lambda z)$, and given the mass densities $\rho(x, y)$ and $\rho'(x', y')$ such that $\frac{\rho(x, y)}{M} = \lambda^3 \frac{\rho'(x', y')}{M'}$, this condition guarantees that $\chi = \chi'$ and $\tilde{I}_{CM} = \tilde{I}'_{CM}$, then the dynamic behavior of the cylinders are equivalent. Since the cylinder's dynamics is basically ruled by the two parameters χ and \tilde{I}_{CM} , we will propose a particular construction of a cylinder which will be characterized by other two parameters, where one of them can be chosen as being the parameter χ , and the second one will be related to the parameter \tilde{I}_{CM} .

In the Fig. 2, we show a cross section of our cylinder model, which consists of a thin cylindrical shell of mass m_C with uniform mass distribution, attached to a mass line m_P , parallel to the cylinder's principal axis. Besides the theoretical importance of this cylinder model that will be used in the presentation of our main results, this model could also be used for an experimental study of the jump effect.

Let us argue that this cylinder model encompasses all possible cases of general eccentric cylinders characterized by the parameters χ and \tilde{I}_{CM} . Note that the mass of the cylinder model is given by $M = m_C + m_P$. Aside the parameter $\chi = d/R$, where R is the radius of the thin cylindrical shell, we introduce the parameter $k_m = m_C/M$.

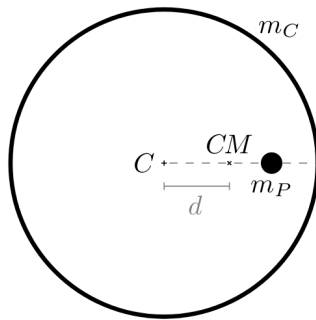


Figure 2: Cross section of a thin cylindrical shell of mass m_C plus a mass line m_P parallel to the cylinder's principal axis.

For example, some particular cases are:

- One where CM coincides with C , so we have $d = 0$ (namely $\chi = 0$), this case happens when the mass line m_P passes through C . The parameter k_m controls the different possibilities for the values of the moment of inertia.
- One where CM is over the border of the cylinder, it means $d = R$, this case happens when $\chi = 1$ and $k_m = 0$.

Through the relation that defines the CM , we can show that the distance s between the CM and the mass line m_P , is given by $s = \frac{k_m}{1-k_m}\chi R$. Then the moment of inertia I_C is computed as follows

$$\begin{aligned} I_C &= m_C R^2 + m_P (d + s)^2 = m_C R^2 + \frac{M^2}{m_P} d^2, \\ \Rightarrow \frac{I_C}{MR^2} &= k_m + \frac{\chi^2}{1 - k_m}. \end{aligned} \quad (17)$$

Since $Md^2 \leq I_C \leq MR^2$, we have that: $\chi^2 \leq \frac{I_C}{MR^2} \leq 1$, and therefore $0 \leq \chi \leq 1$. Then from Eq. (17), we have that $0 \leq k_m \leq 1 - \chi$. Moreover, according to Eq. (17) for the different values of χ and k_m in the former intervals, we cover all the possible values for $\frac{I_C}{MR^2}$. From Eq. (17), we have that $\tilde{I}_{CM} = \frac{I_{CM}}{MR^2} = k_m + \frac{k_m \chi^2}{1 - k_m}$, where this parameter \tilde{I}_{CM} appears in Eq. (16), which explicitly exhibits the independence of the dynamics in relation to the mass M and the radius R when χ and k_m are fixed.

3 Conditions for a slip-free transition from pure rolling to flight motion

As mentioned in the previous section, the cylinder whole motion is basically composed of three types of particular motions: pure rolling, rolling plus slipping and flight motion. From results of numerical simulation (work in progress [22]), we have observed that depending on the initial conditions, the values of the parameters χ , k_m and the ramp inclination α , the cylinder performs a variety of interesting motions. The most common situation corresponds to the case where the cylinder initially performs a pure rolling motion, then the motion is alternated between pure rolling and rolling plus slipping, until at some point the cylinder loses contact with the ramp and jumps.

In this section, we will study the following sequence of motions for the cylinder and the conditions required to have such a sequence.

$$\begin{aligned} \theta &= \theta_0 \Rightarrow \text{initial position,} \\ \theta_0 &< \theta < \theta_J \Rightarrow \text{pure rolling motion,} \\ \theta &= \theta_J \Rightarrow \text{jump position,} \\ \theta &> \theta_J \Rightarrow \text{flight motion.} \end{aligned}$$

Note that the transition from pure rolling to flight motion happens at the point where $\theta = \theta_J$. The subscript J means that we are considering the value of the quantities at the instant of the jump. From here to the rest of the paper, we will use the following acronym JARM to mean: jump after a pure rolling motion.

As discussed in section 2, at the point where the cylinder jumps, the angle θ and the angular velocity $\dot{\theta}$ must satisfy Eq. (14). We have denoted by θ_J the angle that is a solution of Eq. (14). Therefore from this equation, we can write

$$\dot{\theta}_J^2 = \frac{g \cos \alpha}{d \cos \theta_J}. \quad (18)$$

Substituting Eq. (18) into the equation of motion Eq. (11), we obtain

$$\ddot{\theta}_J = \frac{g(1 + \chi \cos \theta_J) \sec \theta_J \sin(\alpha + \theta_J)}{R \left(k_m + \frac{\chi^2}{1-k_m} + 1 + 2\chi \cos \theta_J \right)}. \quad (19)$$

In order to have a JARM, since by definition the cylinder does not slip, the force of friction between the cylinder and the ramp should be static, and

$$\left| \frac{F_x}{F_y} \right| \leq \mu_s, \quad (20)$$

where F_x and F_y are the friction and normal force, respectively. Remember that the definition of these forces as given in Eqs. (9) are valid for general rolling motions (pure rolling or rolling plus slipping). In order to restrict our analysis to the pure rolling motion, we should substitute the equations $\ddot{b} = 0$ and $\ddot{l} = R\ddot{\theta}$, into Eqs. (9); after such substitution, we obtain

$$\begin{aligned} F_x &= MR \left(-\frac{g}{R} \sin \alpha - \chi \dot{\theta}^2 \sin \theta + (1 + \chi \cos \theta) \ddot{\theta} \right), \\ F_y &= MR \left(\frac{g}{R} \cos \alpha - \chi \dot{\theta}^2 \cos \theta - \chi \ddot{\theta} \sin \theta \right). \end{aligned} \quad (21)$$

It is interesting to note that at the beginning of the cylinder's motion, the kinetic energy is low (or zero if the cylinder is left from rest), and the CM of the cylinder is in a higher position so that this initial configuration allows the cylinder to roll down. Clearly at the beginning, F_y is positive because it is dominated by the term $Mg \cos \alpha$, subsequently the values of $\dot{\theta}$ and $\ddot{\theta}$ grow and so the value of the normal force approaches to zero and at some point becomes negative. Since the cylinder is not attached to the ramp, negative values of the normal force are not physical allowed in our study.

Before the normal force becomes negative (when it is positive and approaching zero), the inequality given by Eq. (20) is satisfied. However, at some point, this inequality will no longer hold, which means that the cylinder will begin to slip. Numerical inspection [22] has revealed that the point where inequality (20) is no longer valid is located in proximity to two other points: the point where the normal force becomes zero and the point where the jump condition is satisfied (as given by Eq. (14)). Based on these observations, and in order to have a JARM in the case of pure rolling motion, we will analyze the following condition for the normal force:

$$F_y > 0. \quad (22)$$

Since this condition is less restrictive than the condition given by Eq. (20), it is clear that we will need to complement Eq. (22) with Eq. (20).

3.1 Conditions for a JARM independent of the initial conditions

In order to perform a general analysis of the values and signs of the friction and normal force at the jump point, namely when $\theta = \theta_J$, we substitute Eqs. (18) and (19) into Eqs. (21), so that we obtain

$$F_{x,J} = -\frac{gM \left(k_m + \frac{\chi^2}{1-k_m} - \chi^2 \cos^2 \theta_J \right) \sec \theta_J \sin(\alpha + \theta_J)}{k_m + \frac{\chi^2}{1-k_m} + 1 + 2\chi \cos \theta_J}, \quad (23)$$

$$F_{y,J} = -\frac{gM \chi (1 + \chi \cos \theta_J) \tan \theta_J \sin(\alpha + \theta_J)}{k_m + \frac{\chi^2}{1-k_m} + 1 + 2\chi \cos \theta_J}. \quad (24)$$

Regarding the result of the normal force $F_{y,J}$ from equation (24), we note that $F_{y,J}$ is not necessarily equal to zero. In the case where $F_{y,J} > 0$, and since for $\theta > \theta_J$ we have $F_y = 0$, it is clear that

the normal force changes discontinuously from a non-vanishing to zero value at the point where the cylinder jumps.

Note that some terms in Eqs. (23) and (24) are positive, these are: $k_m + \frac{\chi^2}{1-k_m} + 1 + 2\chi \cos \theta_J > 0$; and $1 + \chi \cos \theta_J > 0$. Also from Eq. (18) we have: $\cos \theta_J > 0$; and thus $k_m + \frac{\chi^2}{1-k_m} - \chi^2 \cos^2 \theta_J > 0$. After consideration of the positivity condition of these terms, employing Eqs. (23) and (24), we get

$$\text{sign}(F_{x,J}) = -\text{sign}(\sin(\alpha + \theta_J)), \quad (25)$$

$$\text{sign}(F_{y,J}) = -\text{sign}(\sin \theta_J \sin(\alpha + \theta_J)). \quad (26)$$

A subtle issue that can be observed from equation (26) is that the normal force at the jump point could even be negative. Physically, this would mean that before the cylinder jumps, the normal force could have been zero. Therefore, the cylinder may have slipped before jumping, implying that the pure rolling assumption is no longer valid. In what follows, we will address this issue in more detail.

As mentioned before, in order to have a JARM, the condition that the normal force should be positive needs to be complemented with Eq. (20). Therefore, let us start our analysis by searching for possible allowed values of θ_J through Eq. (26), so that the condition given by Eq. (22) is satisfied. In that sense, it is not difficult to show that

$$2\pi n - \alpha < \theta_J < 2\pi n, \quad n = 1, 2, 3, \dots \quad (27)$$

From Fig. 3a, we can see that the angle $\alpha + \theta$ is measured between \vec{d} and the vertical line. Therefore from this geometrical configuration of the angles, we can easily prove that the whole shadowed regions (gray and green) corresponds to the regions where $\cos \theta > 0$. Now from Eq. (26), it is not difficult to see that in the gray region $F_{y,J} < 0$, and in the green region $F_{y,J} > 0$.

Therefore, the only domain where a JARM could happen (due to the condition in Eq. (22)), is when the CM is inside the green region, on the other regions a JARM is precluded. Notice that the green region agrees with the interval for θ_J given by Eq. (27), where the integer number n is interpreted as the counting of the full turns completed by the cylinder. Finally, in the green region we can check that $F_{x,J} < 0$ (this result is obtained from Eq. (25)), which means that the static friction force over the cylinder points along and upward the ramp.

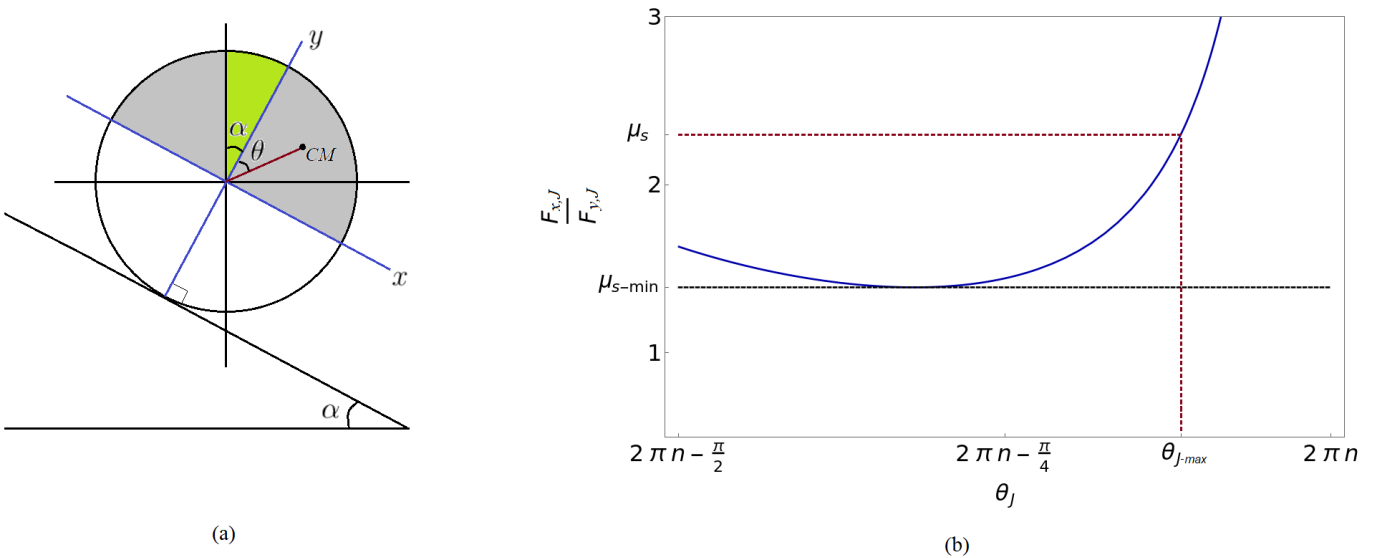


Figure 3: (a) Representation of the angles α and θ on the cross section of the cylinder. (b) Plot of the function $\mu(\chi, k_m, \theta_J)$, for $\chi = 0.5$ and $k_m = 0.4$.

More restrictions for the possible allowed values of θ_J can be obtained from the condition given

by Eq. (20). So, substituting Eqs. (23) and (24) into Eq. (20) we obtain

$$\mu(\chi, k_m, \theta_J) \equiv \frac{\frac{-k_m^2 + k_m + \chi^2}{(k_m - 1)\chi^2} + \cos^2 \theta_J}{\sin \theta_J \left(\frac{1}{\chi} + \cos \theta_J \right)} \leq \mu_s. \quad (28)$$

In the Fig. 3b, a typical plot of the function $\mu(\chi, k_m, \theta_J)$ is shown. By fixing the value of μ_s , and using the inequality given in Eq. (28), we can calculate the region to which θ_J belongs. It is worth noting that the domain of θ_J as shown in Fig. 3b is bigger than the one defined by Eq. (27), however it is important to keep in mind that the lower bound for θ_J must be greater than or equal to $2\pi n - \alpha$. We also note that due to the usual periodic property of the trigonometric functions that appear in $\mu(\chi, k_m, \theta_J)$, the plot of this function is the same for any integer value n . After some analysis of the Fig. 3b, we conclude that to have a JARM:

1. There is a minimum value μ_{s-min} for the coefficient of static friction.
2. For each $\mu_s > \mu_{s-min}$, we have that $\max\{2\pi n - \alpha, \theta_{J-min}\} < \theta_J < \theta_{J-max}$; where θ_{J-min} and θ_{J-max} are identified as follows, when $\mu_s > \mu_{s-min}$ and $\mu_s \approx \mu_{s-min}$, there are two solutions to the equation $\mu(\chi, k_m, \theta_J) = \mu_s$, these solutions are precisely θ_{J-min} and θ_{J-max} , while for values of μ_s such that $\mu_s \gg \mu_{s-min}$, there is only one solution that is θ_{J-max} .
3. Since there is a maximum value for θ_J , which was denoted by θ_{J-max} , then there is a minimum value for α , denoted by α_{min} which satisfies $\alpha_{min} = 2\pi n - \theta_{J-max}$, this is true because θ_J satisfies the inequality given in Eq. (27).

As a specific application of the general results presented above, let us consider the case where $\alpha = 0$, which corresponds to the horizontal plane. From Eq. (27), we can see that the only valid value for the angle θ_J in this case is $\theta_J = 2\pi n$. However, substituting this value into the left-hand side of Eq. (28) results in a divergence, indicating that to maintain roll without slipping, the coefficient of static friction μ_s must approach infinity. Since such a value is physically impossible, we can conclude that the no-slip condition must be violated before the cylinder jumps, regardless of the values of χ and k_m . In the following discussion, we will consider the case where $\alpha \neq 0$.

3.2 Conditions for a JARM using initial conditions

Our study in the previous subsection is interesting because it proves that there are restrictions for the possible allowed values of α , μ_s and θ_J . Also note that to derive our previous results, we have not used any particular initial condition.

In this subsection, we consider the following quite standard initial conditions: the cylinder is left from rest $\dot{\theta}_0 = 0$ at the top of the ramp, with $\theta_0 = 0$. As we are going to see, the setting of these initial conditions will further restrict the existence of a JARM.

Using the conservation of energy, which is valid for pure rolling motion, together with the initial conditions $\dot{\theta}_0 = 0$ and $\theta_0 = 0$, from the jump condition given by Eq. (14), we can show that the angle θ_J at the jump point is the root of the function:

$$J(\theta) = -1 + \frac{(\chi \cos \alpha - \chi \cos(\alpha + \theta) + \theta \sin \alpha) \cos \theta}{(2\pi\gamma + \cos \theta - 1) \cos \alpha}, \quad (29)$$

where the parameter γ is defined by

$$\gamma = \frac{k_m^2 + 2k_m\chi - \chi^2 - 2\chi - 1}{4\pi(k_m - 1)\chi}. \quad (30)$$

Let us provide conditions for the existence of roots θ_J of the function $J(\theta)$ with the restriction given by equation (27). It turns out that to guarantee the existence of a root $\theta_J \in [2\pi n - \alpha, 2\pi n]$ of the function $J(\theta)$, we must have that

$$J(2\pi n - \alpha) = \left(\frac{\chi \cos \alpha + (2\pi n - \alpha) \sin \alpha - \chi}{\cos \alpha + 2\pi\gamma - 1} - 1 \right) < 0, \quad \text{and}, \quad (31)$$

$$J(2\pi n) = \left(\frac{n \tan \alpha}{\gamma} - 1 \right) > 0. \quad (32)$$

Note that through the equation: $J(\theta_J) = 0$, it should be possible to express θ_J as a function of the parameters α , χ , and k_m , namely

$$\theta_J = \theta_{n,J}(\alpha, \chi, k_m), \quad (33)$$

where the subscript n explicitly indicates that θ_J belongs to the interval $[2\pi n - \alpha, 2\pi n]$. Using this equation (33), we can write the inequality (28) as follows

$$\frac{\frac{-k_m^2 + k_m + \chi^2}{(k_m - 1)\chi^2} + \cos^2(\theta_{n,J}(\alpha, \chi, k_m))}{\sin(\theta_{n,J}(\alpha, \chi, k_m)) \left[\frac{1}{\chi} + \cos(\theta_{n,J}(\alpha, \chi, k_m)) \right]} \leq \mu_s. \quad (34)$$

We could think that for given values of n , α , χ , k_m and μ_s such that inequalities (31), (32) and (34) are true, it would be enough to guarantee that the cylinder will jump without first having slipped. However, note that the above analysis has been performed at the point where the cylinder jumps, namely the inequalities (31), (32) and (34) do not necessarily guarantee pure rolling motion for values of the angle θ such that $\theta < \theta_J$. Therefore we will need to impose more restrictions.

Since extra conditions will come from the analysis of inequalities of the type given in (22) and (20), we need to write F_x and F_y for generic values of θ such that $\theta < \theta_J$. These components of the force are given by Eqs. (21).

For the initial conditions $\dot{\theta}_0 = 0$ and $\theta_0 = 0$, using the equation of motion (11), and the conservation of the energy, we can express the angular velocity $\dot{\theta}$ and the angular acceleration $\ddot{\theta}$ in terms of the angle θ , so that the components of the force given in Eqs. (21) can be written as functions that depend explicitly on θ

$$F_x(\theta) = - \frac{gM}{4\chi(2\pi\gamma + \cos \theta - 1)^2} \left[\sin \alpha (16\pi^2\gamma^2\chi - 16\pi\gamma\chi - 4\pi\gamma - \chi^2 + 3\chi + 2 \right. \\ + 2\pi\gamma\chi^2 + 2(-1 + (-3 + 6\pi\gamma)\chi) \cos \theta + \chi \cos(2\theta) - 2\theta \sin \theta - 4\theta\chi \sin \theta \\ + 8\pi\gamma\theta\chi \sin \theta + \theta\chi \sin(2\theta)) + \chi(2 \cos \alpha(-1 - 2\chi + 4\pi\gamma\chi + \chi \cos \theta) \sin \theta \\ \left. - (-2 + 4\pi\gamma + \chi) \sin(\alpha + \theta) - \chi((-3 + 6\pi\gamma) \sin(\alpha + 2\theta) + \sin(\alpha + 3\theta)) \right], \quad (35)$$

$$F_y(\theta) = \frac{gM}{4(2\pi\gamma + \cos \theta - 1)^2} \left[\cos \alpha (6 - 16\pi\gamma + 16\pi^2\gamma^2 - 4\chi + 2\pi\gamma\chi \right. \\ + (-8 - 8\pi\gamma(-2 + \chi) + 7\chi) \cos \theta + (2 - 4\chi + 6\pi\gamma\chi) \cos(2\theta) + \chi \cos(3\theta)) \\ - \sin \alpha (3\theta + 4(-1 + 2\pi\gamma)\theta \cos \theta + \theta \cos(2\theta) - 2\sin \theta + 4\pi\gamma \sin \theta \\ \left. + 3\chi \sin \theta + \sin(2\theta) - 3\chi \sin(2\theta) + 6\pi\gamma\chi \sin(2\theta) + \chi \sin(3\theta)) \right]. \quad (36)$$

In order to guarantee a pure rolling motion throughout the entire path from $\theta = 0$ to the point where the cylinder jumps $\theta = \theta_J$, for any value of θ such that $0 < \theta < \theta_J$, the following inequalities must be satisfied

$$F_y(\theta) > 0, \quad \text{and}, \quad (37)$$

$$\frac{|F_x(\theta)|}{F_y(\theta)} \leq \mu_s. \quad (38)$$

Let us summarize the main result of this subsection. We have shown that using the initial conditions $\theta_0 = 0$ and $\dot{\theta}_0 = 0$, to have a JARM the parameters n , α , χ , k_m and μ_s need to be chosen such that the inequalities (31), (32), (34), (37) and (38) are satisfied. Therefore, this result imposes nontrivial restrictions on the possible allowed values of the parameters that appear in the equations of the problem.

3.3 Regions in the parameter space (α, χ, k_m) for fixed values of n and μ_s

In order to have a JARM for the initial conditions $\theta_0 = 0$ and $\dot{\theta}_0 = 0$, in this subsection, we are going to show the region where the parameters must belong. Since essentially we have five parameters n , μ_s , α , χ , and k_m to visualize the region defined by the inequalities (31), (32), (34), (37) and (38), we will need to fix at least two parameters so that the remaining three parameters can be visualized in a three-dimensional space.

By fixing the value of the parameters n and μ_s , in Fig. 4 we present the regions in the parameter space (α, χ, k_m) where the inequalities mentioned in the previous paragraph are fulfilled, namely if we choose any set of parameters α , χ , and k_m that belong to these regions, we guarantee the occurrence of a JARM. Comparing Fig. 4(b) and Fig. 4(a), we see that the regions with $\mu_s = 1$ are bigger than the regions with $\mu_s = 0.7$. This result makes sense since for a larger static coefficient of friction, we expect that the cylinder has more chances to maintain pure rolling motion.

For a fixed value of μ_s , we can also compare the regions obtained with different values of n . For instance, from Fig. 4(a), for the value of $\mu_s = 0.7$, we observe that as the values of n increase, the corresponding regions are getting smaller. In general, for any value of μ_s , this pattern was observed. The physical interpretation of this result is as follows, first let us remember that n represents the number of turns performed by the cylinder, so for a given value of μ_s , since $n = 1$ is the lowest possible value for n , the greatest chance of having a JARM occurs before the cylinder completes a full turn, and the chance decreases every time we increase the value of n .

Regarding the inclination of the ramp given by the angle α (where $\pi/2$ is its maximum value), we observed that, inside the regions shown in Fig. 4, large values of α are in correspondence with small values of χ . This type of correspondence makes sense since for a high inclination of the ramp, in order to avoid a slipping, the normal force should not oscillate too much, and that happens when the value of χ is small.

When the inclination of the ramp gets closer to the value of $\pi/2$, we notice that the regions defined by the values of χ and k_m become smaller, where in the limit case $\alpha \rightarrow \pi/2$ the parameters χ and k_m vanish. This is evidenced by the fact that when α is close to $\pi/2$, the region where a JARM occurs has the shape of a wedge where its vertex is given by the point $\alpha = \pi/2$, $\chi = 0$ and $k_m = 0$. In order to interpret this result, let us remember that inside the region where a JARM happens, large values of α are in correspondence with small values of χ , namely when the CM is close to the geometric center C of the cylinder, there are less oscillations of the normal force, which implies in less chances to have a slip. We conclude that high values of α are allowed provided that the parameters χ and k_m are small enough. Therefore, an unexpected result of having a JARM is obtained in the limit case where $\alpha \rightarrow \pi/2$, $\chi \rightarrow 0$ and $k_m \rightarrow 0$.

4 Summary and discussion

For a given value of the coefficient of static friction μ_s , we have shown that a general eccentric cylinder performs a jump starting from pure rolling motion, provided that the angle α , and the parameters χ and k_m that characterize the cylinder, belong to a restricted region. If these parameters do not belong to the aforementioned region, the cylinder has to perform another type of motion, such as slipping with rolling, before the jump. In a future paper [22], we will analyze these other varieties of motion using our general cylinder.

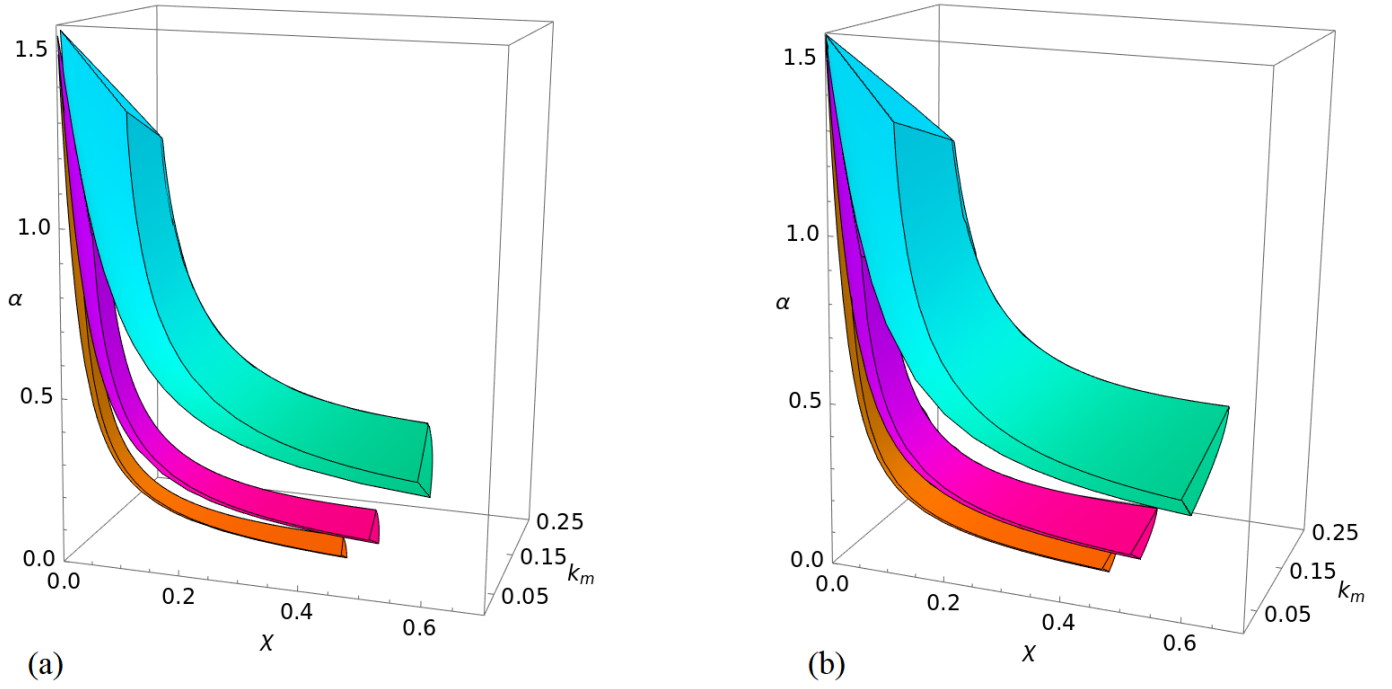


Figure 4: Regions where a JARM happens in the space of parameters α , χ and k_m , for fixed values of μ_s , n and the initial conditions $\theta_0 = 0$ and $\dot{\theta}_0 = 0$. (a) Here we have set $\mu_s = 0.7$ and $n = 1, 2, 3$ correspond to the green, purple and orange solids respectively. (b) This plot is the same as the one presented in (a) but with $\mu_s = 1$.

Another important issue that can be explored is related to the initial conditions. We have presented a general discussion about the existence of JARM that is independent of the initial conditions. As a result of this analysis, we show that the value of the angle θ_J is restricted to some interval. To fix the value of θ_J , some particular initial conditions are needed. Therefore, we have used the somewhat standard initial conditions, $\theta_0 = 0$ and $\dot{\theta}_0 = 0$. It will be an interesting and non-trivial problem to analyze how the regions shown in Fig. 4 change when other initial conditions are used. For example, we can see if these regions increase or decrease, which would physically imply a greater or lesser chance of having JARM. What would be the optimal initial conditions that allow a greater chance of having JARM?

Finally, since only the slipping motion before the jump has been observed in experiments and theoretical studies carried out to date, it has been a common conclusion that the no-slip conditions must be violated before the jump. Indeed, when $\alpha = 0$, on general grounds, we have definitely shown that this last conclusion is true. However, in the case where $\alpha \neq 0$, there is a chance to have JARM. Therefore, to empirically test the occurrence of JARM, it would be important to set up an experiment that takes into account appropriate values for μ_s and the parameters χ and k_m .

Acknowledgements

We would like to thank Dominique Sugny, Gabriela and Pavao Mardešić for useful discussions.

References

- [1] J. E. Littlewood, *A mathematician's miscellany*. Methuen, 1953.
- [2] T. F. Tokieda, “The hopping hoop,” *The American Mathematical Monthly*, vol. 104, no. 2, pp. 152–154, 1997.

- [3] J. P. Butler, “Hopping hoops don’t hop,” *The American Mathematical Monthly*, vol. 106, no. 6, pp. 565–568, 1999.
- [4] T. Pritchett, “The hopping hoop revisited,” *The American Mathematical Monthly*, vol. 106, no. 7, pp. 609–617, 1999.
- [5] L. Yanzhu and X. Yun, “Qualitative analysis of a rolling hoop with mass unbalance,” *Acta Mechanica Sinica*, vol. 20, no. 6, pp. 672–675, 2004.
- [6] W. F. D. Theron, “The rolling motion of an eccentrically loaded wheel,” *American Journal of Physics*, vol. 68, no. 9, pp. 812–820, 2000.
- [7] A. Taylor and M. Fehrs, “The dynamics of an eccentrically loaded hoop,” *American Journal of Physics*, vol. 78, no. 5, pp. 496–498, 2010.
- [8] A. Bronars and O. M. O’Reilly, “Gliding motions of a rigid body: the curious dynamics of littlewood’s rolling hoop,” *Proceedings of the Royal Society A: Mathematical, Physical and Engineering Sciences*, vol. 475, no. 2231, p. 20190440, 2019.
- [9] M. Batista, “Self-induced jumping of a rigid body of revolution on a smooth horizontal surface,” *International Journal of Non-Linear Mechanics*, vol. 43, no. 1, pp. 26–35, 2008.
- [10] A. P. Ivanov, “On detachment conditions in the problem on the motion of a rigid body on a rough plane,” *Regular and Chaotic Dynamics*, vol. 13, no. 4, pp. 355–368, 2008.
- [11] Y. Shimomura, M. Branicki, and H. Moffatt, “Dynamics of an axisymmetric body spinning on a horizontal surface. ii. self-induced jumping,” *Proceedings of the Royal Society A: Mathematical, Physical and Engineering Sciences*, vol. 461, no. 2058, pp. 1753–1774, 2005.
- [12] P. Kessler and O. M. O’Reilly, “The ringing of euler’s disk,” *Regular and Chaotic dynamics*, vol. 7, no. 1, pp. 49–60, 2002.
- [13] R. I. Leine, “Experimental and theoretical investigation of the energy dissipation of a rolling disk during its final stage of motion,” *Archive of Applied Mechanics*, vol. 79, no. 11, pp. 1063–1082, 2009.
- [14] W. Theron and M. Maritz, “The amazing variety of motions of a loaded hoop,” *Mathematical and Computer Modelling*, vol. 47, no. 9, pp. 1077–1088, 2008.
- [15] P. Onorato, M. Malgieri, P. Mascheretti, and A. D. Ambrosio, “The surprising rolling spool: librational motion and failure of the pure rolling condition,” *European Journal of Physics*, vol. 36, p. 038002, mar 2015.
- [16] S. A. Moore, D. Culver, and B. P. Mann, “The eccentric disk and its eccentric behavior,” *European Journal of Physics*, vol. 42, p. 065012, oct 2021.
- [17] A. Carnevali and R. May, “Rolling motion of non-axisymmetric cylinders,” *American Journal of Physics*, vol. 73, no. 10, pp. 909–913, 2005.
- [18] L. Turner and A. M. Turner, “Asymmetric rolling bodies and the phantom torque,” *American Journal of Physics*, vol. 78, no. 9, pp. 905–908, 2010.
- [19] J. H. Jensen, “Rules for rolling as a rotation about the instantaneous point of contact,” *European Journal of Physics*, vol. 32, pp. 389–397, jan 2011.
- [20] B. Y.-K. Hu, “Rolling of asymmetric discs on an inclined plane,” *European Journal of Physics*, vol. 32, pp. L51–L54, oct 2011.

- [21] R. W. Gómez, J. J. Hernández-Gómez, and V. Marquina, “A jumping cylinder on an inclined plane,” *European Journal of Physics*, vol. 33, pp. 1359–1365, jul 2012.
- [22] E. A. Arroyo and et. al., “work in progress.”